Quantum Optimization of Reconfigurable Intelligent Surfaces for Mitigating Multipath Fading in Wireless Networks

Emanuel Colella, *Graduate Student Member, IEEE*, Luca Bastianelli, *Member, IEEE*, Valter Mariani Primiani, *Senior Member, IEEE*, Zhen Peng, *Senior Member, IEEE*, Franco Moglie, *Senior Member, IEEE*, and Gabriele Gradoni, *Senior Member, IEEE*

***Abstract*—Wireless communication technology has become important in modern life. Real-world radio environments present significant challenges, particularly concerning latency and multipath fading. A promising solution is represented by reconfigurable intelligent surfaces (RIS), which can manipulate electromagnetic waves to enhance transmission quality. In this study, we introduce a novel approach that employs the quantum approximate optimization algorithm (QAOA) to efficiently configure RIS in multipath environments. Applying the spin glass (SG) theoretical framework to describe chaotic systems, along with a variable noise model, we propose a quantum-based minimization algorithm to optimize RIS in various electromagnetic scenarios affected by multipath fading. The method involves training a parameterized quantum circuit using a mathematical model that scales with the size of the RIS. When applied to different EM scenarios, it directly identifies the optimal RIS configuration. This approach eliminates the need for large datasets for training, validation, and testing, streamlines, and accelerates the training process. Furthermore, the algorithm will not need to be rerun for each individual scenario. In particular, our analysis considers a system with one transmitting antenna, multiple receiving antennas, and varying noise levels. The results show that QAOA enhances the performance of RIS in both noise-free and noisy environments, highlighting the potential of quantum computing to address the complexities of RIS optimization and improve the performance of the wireless network.**

***Index Terms*—6G, fast fading, ising model, metamaterials, optimization, quantum computing, reconfigurable intelligent surface, wireless communication.**

Received 31 July 2024; revised 20 September 2024; accepted 31 October 2024. Date of publication 7 November 2024; date of current version 25 November 2024. This work was supported by the UKRI Research grant EP/X038491/1 under Grant ECCS-EPSRC Collaboration Scheme on "Towards Quantum-Assisted Reconfigurable Indoor Wireless Environments" *(Corresponding author: Emanuel Colella.)*

Emanuel Colella, Luca Bastianelli, Valter Mariani Primiani, and Franco Moglie are with the Dipartimento di Ingegneria dell'Informazione, Università Politecnica delle Marche, 60131 Ancona, Italy, and also with the Consorzio Nazionale Interuniversitario per le Telecomunicazioni, 43124 Parma, Italy (e-mail: e.colella@pm.univpm.it; l.bastianelli@pm.univpm.it; v.mariani@univpm.it; f.moglie@univpm.it).

Zhen Peng is with the Center for Computational Electromagnetics, Department of Electrical and Computer Engineering, University of Illinois at Urbana-Champaign, Urbana, IL 61801 USA (e-mail: zvpeng@illinois.edu).

Gabriele Gradoni is with the University of Surrey, GU2 7XH Guildford, U.K., and also with the University of Cambridge, CB2 1TN Cambridge, U.K. (e-mail: g.gradoni@surrey.ac.uk).

Digital Object Identifier 10.1109/JMMCT.2024.3494037

I. Introduction

IN TODAY'S technological landscape, wireless communication technology plays a central role in every aspect of our daily lives [1], [2]. From mobile devices to Wi-Fi networks, from satellite communications to IoT devices, wireless connectivity has changed the way of communicating [3], [4]. These technologies face significant challenges, including latency, reliability and multipath fading causing unpredictable variation in received signal intensity and data loss during transmission [5], [6], [7]. To address the problem of multipath fading and improve the performance of wireless networks, several innovative solutions have been proposed, including RISs [8], [9]. RIS are configurable EM surfaces consisting of controllable elements, which can be reconfigured to manipulate the behavior of the EM waves, reducing the effect of multipath fading and increasing the intensity of the received signal [10], [11], [12], [13], [14]. One of the main challenges facing RIS lies above the optimization. Currently, several classical solutions are proposed to find the optimal cell configuration that maximize the intensity of the received signal [15]. Some common approaches include convex optimization algorithms, genetic algorithms and artificial intelligence algorithms to improve the reception performances [16], [17]. A mathematical model describing the behavior of disordered magnetic systems has been proposed by Giorgio Parisi in 1980 to study the behavior of spin glasses (SGs) [18], [19]. This model is a Hamiltonian widely used to optimize magnetic disordered systems in which particles interact to produce magnetic configuration that minimize the energy of the system [20], [21], [22]. This model can be used to describe the behavior of a RIS of N transmitting antennas in the presence of multipath fading and P receiving antennas. The solution of this model allows to find the configuration of the RIS that maximizes the intensity of the received signal in presence of noise [23]. Nowadays, the advent of quantum computers is receiving more and more attention from the scientific community, marking a revolution in the computer science field [24], [25]. This interest has led to the development of quantum algorithms that allow the principles of quantum mechanics to be exploited to reach performances that cannot be obtained by classical computers [26], [27]. Among the broad spectrum of quantum algorithms, a class of variational quantum algorithms (VQAs) have received significant attention due to

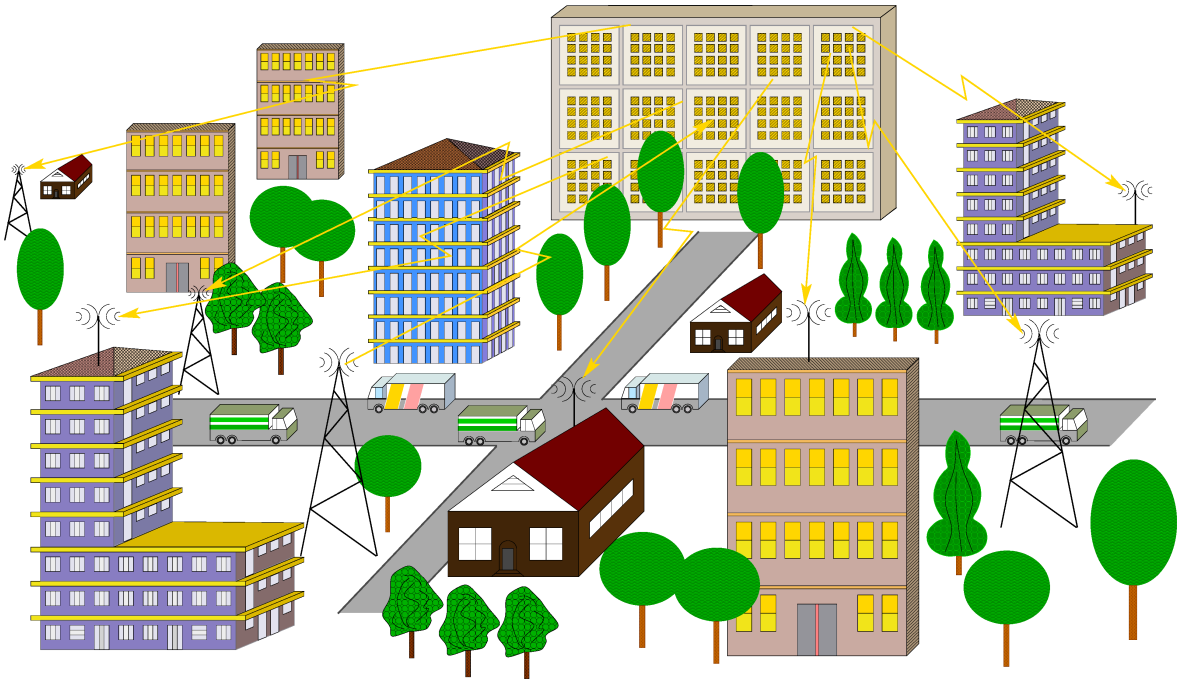

Fig. 1. RIS within a smart radio environments. The system consists of a single transmitting RIS and P receiving antenna. The RIS reconfigures itself to maximize the overall intensity of the received signal.

their ability to overcome quantum hardware limitations such as circuit depth, number of qubits, and noise of near intermediate scale quantum (NISQ) computers [28], [29]. The VQAs are a class of hybrid classical-quantum algorithms that combine elements of quantum computing with classical optimization techniques to solve optimization problems [30], [31]. One of the most promising VQA to address optimization problems is the quantum approximate optimization algorithm (QAOA) [32]. The QAOA aims to find approximate solutions to combinatorial optimization problems by minimizing an objective function to approximate optimal solution of physical system. As shown by [33], QAOA does not require any training, validation and test data to be trained, it just employs a mathematical model that is scalable with the RIS dimension. Therefore, the objective of this paper, is to apply the QAOA for RIS optimization in order to find optimal RIS configuration in any possible disordered scenarios governed by the SG Hamiltonian in presence of multipath fading as N and P vary as an extension of [34]. Unlike classical optimization algorithms, QAOA leverages the power of quantum mechanical principles to handle the exponential growth of the RIS configurations. This enables QAOA to identify the best RIS configuration much more quickly, without the need to run optimization routines for every single scenario, so significantly reducing the computational times. The results of this study open up possibilities for future innovations in large-dimensional RIS optimization that can be solved using the power of quantum computing in smart radio environments.

II. RIS Model Based on the Spin Glasses Hamiltonian

RISs are intelligent devices that control the propagation of EM waves in wireless communication systems. Considering the system of a RIS of N cells (transmitting elements) and P receiving antennas (see Fig. 1), the objective of the RIS is to maximize the overall intensity $\mathcal{I}$ of the signal received to P antennas:

$$\mathcal{I} = \sum_{\tau=1}^{P} \mathcal{I}^{(\tau)} \tag{1}$$

The single target contribution $\mathcal{I}^{(\tau)}$ reads as follows:

$$\mathcal{I}^{(\tau)} = \sum_{i,j}^{N} \left|\xi_i^{(\tau)}\right| \left|\xi_j^{(\tau)}\right| A_i A_j e^{\imath\left(\arg \xi_i^{(\tau)} - \arg \xi_j^{(\tau)} + \phi_i - \phi_j\right)} \tag{2}$$

where $\xi_i^{(\tau)} = |\xi_i^{\tau}| e^{\imath \arg \xi_i^{(\tau)}}$ are the complex transmission matrix elements [35] from the i-th incoming beam to the target τ [23]. Each RIS cell can be programmed into a state s_i characterized by a phase factor $\phi_i = \pm\pi$ of the transmitted wave, equivalent to an amplitude factor of $s_i \in \{-1, 1\}$, so that the intensity of a single target (2) can be expressed as

$$\mathcal{I}^{(\tau)} = \sum_{ij}^{1,N} \kappa_{ij}^{(\tau)} s_i s_j \tag{3}$$

where the transmission matrix elements ξ and the field amplitudes A are considered in the following coefficient

$$\kappa_{ij}^{(\tau)} \equiv A_i A_j \xi_i^{(\tau)} \bar{\xi}_j^{(\tau)}, \tag{4}$$

where A are the amplitudes of the beams [23]. Considering a Gaussian beam and expanding it to retrieve a homogeneous distribution of the intensity on the RIS cells, it is possible to approximate all of the amplitudes to a unitary constant. Hence, maximizing the overall intensity $\mathcal{I}$ in the P antennas with respect

to the RIS configuration $\boldsymbol{s}$, means minimizing the following Hamiltonian:

$$\mathcal{H}(\boldsymbol{s}) = -\sum_{ij}^{1,N} J_{ij} s_i s_j \tag{5}$$

where J_{ij} is the interaction matrix defined as follows

$$J_{ij} = \frac{1}{N}\sum_{\tau=1}^{P} \xi_i^{(\tau)} \bar{\xi}_j^{(\tau)} \tag{6}$$

with ξ a complex transmission matrix element [23]. Note that $\boldsymbol{s}$ refers to the RIS configuration, while s_i refers to the single RIS cell state. Moreover, the matrix J is a Hermitian matrix, $J_{ij} = J^{\dagger}$. This theoretical model was developed by Giorgio Parisi to analyze the behavior of a spin system as a function of the external temperature. This model represents the mathematical framework in the spin glass (SG) theory that describes highly disordered systems such as highly resonant environments. In particular, the (5) is a generalization to complex continuous valued patterns of the Hopfield model [36], for which the study of Amit et al. [37] predicts the existence of a low-temperature/large-P SG phase. This external temperature represents the environmental disturbance that randomly causes the spins to flip. In our case we will be using this parameter to describe the environmental disturbance due to multipath fading in a wireless communication system. This parameter is not to be confused with the temperature due to the RIS circuits but rather the environment noise due to multipath fading that influences the RIS optimal configuration. It will be implemented in the QAOA representing the error e_g in the noise model.

III. The Quantum Approximation Optimization Algorithm

The QAOA is a hybrid quantum-classical optimization algorithm that harnesses the power of quantum computing to solve complex combinatorial optimization problems. Introduced by Farhi, Goldstone, and Gutmann in 2014, it has attracted significant attention in the quantum research for its potential to solve optimization problems. Some examples are the traveling salesman problem, the graph cutting problem, and other NP-hard problems [33]. In particular, it involves training a parameterized quantum circuit, also called ansatz, by minimizing a given objective function. Unlike classical machine learning approaches that rely on extensive training, validation, and testing data sets to train the model, the QAOA method employs a mathematical function that simplifies and speeds up the training process. In the QAOA, an optimization problem is formulated using a diagonal operator $\hat{\mathcal{C}}$ acting on a quantum state $|\boldsymbol{s}\rangle$:

$$\hat{\mathcal{C}}\,|\boldsymbol{s}\rangle = \mathcal{C}(\boldsymbol{s})\,|\boldsymbol{s}\rangle \tag{7}$$

where $\hat{\mathcal{C}}$ maps a given classical cost function $\mathcal{C}(\boldsymbol{s})$, defined on N-variables $\boldsymbol{s} = (s_1, \ldots, s_n)$, with $s_i \in \{-1, +1\}$. After mapping the cost function into an operator, the QAOA varies the state $|\boldsymbol{s}\rangle$ until the cost function is close to its absolute minimum. The operator $\hat{\mathcal{C}}$ is a measurable physical quantity acting on the state $|\boldsymbol{s}\rangle$. By applying $\hat{\mathcal{C}}$ to $|\boldsymbol{s}\rangle$, the result of the measurement are the eigenvalues $\mathcal{C}(\boldsymbol{s})$ and eigenvectors $|\boldsymbol{s}\rangle$ of $\hat{\mathcal{C}}$ operator. Considering the measured quantity to be the energy of the system, $\hat{\mathcal{C}}$ is the Hamiltonian operator $\hat{\mathcal{H}}$. Applying the Hamiltonian operator to a general state $|\psi\rangle$, the eigenvalues and eigenvectors of $\hat{\mathcal{H}}$ are found associated to the energies E and the configurations $|\psi\rangle$ of the system, respectively:

$$\hat{\mathcal{H}}\,|\psi\rangle = E\,|\psi\rangle\,. \tag{8}$$

This eigenvalue equation is known as the time-independent Schrödinger equation that describes stationary quantum systems. Considering the energy to be measured in (7), the diagonal operator $\hat{\mathcal{C}} \to \hat{\mathcal{H}}$ while the cost function $\mathcal{C}(\boldsymbol{s}) \rightharpoonup \mathcal{H}(\boldsymbol{s})$. The most widely used Hamiltonian operator for the QAOA is the Ising Hamiltonian operator, due to its universality, easy physical interpretation and simple computational implementation [38]. The Ising Hamiltonian operator is given by the linear combination of the Kronecker products of the Z and I unit operators. The Z operator, also known as Pauli z-operator provides the information of the state along z axis of the Bloch sphere [39]. The I operator is the identity matrix that leaves the system unchanged. These operators have the following matrix representation:

$$Z = \begin{pmatrix} 1 & 0 \\ 0 & -1 \end{pmatrix}, \quad I = \begin{pmatrix} 1 & 0 \\ 0 & 1 \end{pmatrix}. \tag{9}$$

The values on the diagonal are the eigenvalues of the operators that are associated to the possible outcomes of a measurement. For the Z operator the outcomes of a measurement are $1, -1$. In quantum computing, these eigenvalues $1, -1$ are associated to the qubit state $|0\rangle, |1\rangle$, respectively. This connection between the eigenvalues of Z, indicated with $z_i \in \{-1, 1\}$ and the values of the variable $s_i \in \{-1, 1\}$ allow to map s_i into qubit eigenvalue z_i and the cost function $\mathcal{H}(\boldsymbol{s})$ to $\mathcal{H}(\boldsymbol{z})$. Therefore, considering the cost function to be associated with energy $\mathcal{C}(\boldsymbol{s}) \to \mathcal{H}(\boldsymbol{s})$ and the cost function variables to be associated with qubit eigenvalues $\boldsymbol{s} \to \boldsymbol{z}$, the (7) becomes:

$$\hat{\mathcal{H}}\,|\boldsymbol{z}\rangle = \mathcal{H}(\boldsymbol{z})\,|\boldsymbol{z}\rangle\,, \tag{10}$$

where $\hat{\mathcal{H}}$ maps a given classical cost function $\mathcal{C}(\boldsymbol{s})$, defined on n-dimensional bitstring with $z_i \in \{-1, +1\}$. The operator $\hat{\mathcal{H}}$ is obtained by replacing the variable s_i with the Z operator and applying the I operator for other qubits:

$$\hat{\mathcal{H}} = \sum_{i=1}^{m} c_{ij} \prod_{j=1}^{n} \mathcal{P}_{ij}, \tag{11}$$

where c_{ij} are the coefficients of the cost function variables, $\mathcal{P}_{ij} \in \{Z, I\}$ is the Kronecker product of the Z and I operators and m is the total number of combinations. To minimize the $\mathcal{H}(\boldsymbol{z})$, a variational state $|\boldsymbol{z}\rangle$ has to be defined. This state will vary until the minimum of the cost function $\mathcal{H}(\boldsymbol{z})$ is reached. This variational state is called Ansatz. A variational state is represented by a parameterized quantum circuit consisting of a sequence of gates with tunable parameters applied to specific qubits. In the QAOA, the Ansatz has a well-defined circuit model consisting of two Hamiltonian operators, the Ising Hamiltonian operator $\hat{\mathcal{H}}_C$ that maps the cost function, and a mixing Hamiltonian operator $\hat{\mathcal{H}}_M$. The subscript $_C$ is used to distinguish it

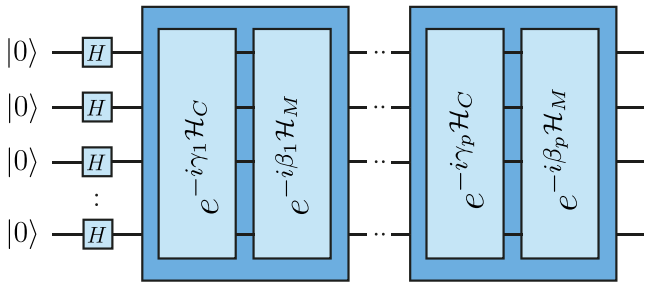

Fig. 2. QAOA Ansatz. It consists of applying the $\mathcal{U}_C$ and $\mathcal{U}_M$ unitary operators to the initial state of n-qubits.

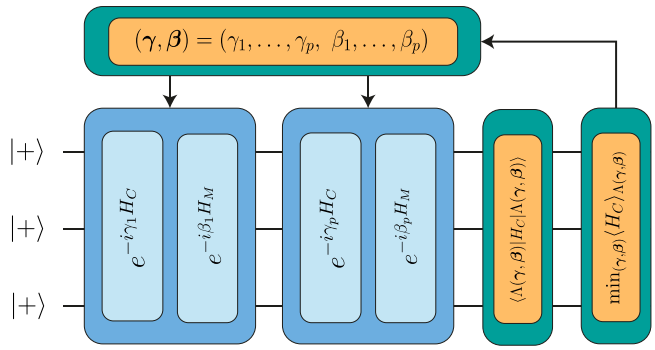

Fig. 3. Block diagram of QAOA algorithm. 1st block shows the initialization of the states of qubit, 2nd block shows the Ansatz definition, 3rd block represents the expectation value computation, 4th block shows the classical optimization of the objective function, 5th shows the update of the circuit parameters after one cycle of optimization process, 6th shows the parameter assignment. These steps repeats until the algorithm converges.

from the mixing Hamiltonian. Note that $\hat{\mathcal{H}}_C \equiv \hat{\mathcal{H}}$. Once the qubits have been initialized in the state $|0\rangle$, the Hadamard gates have been applied. These Hamiltonian operators are applied in succession in the circuit in terms of variational gates as a function of parameters $\boldsymbol{\gamma} = \{\gamma_1, \gamma_2, \ldots, \gamma_p\}$ and $\boldsymbol{\beta} = \{\beta_1, \beta_2, \ldots, \beta_p\}$. The p is the circuit depth and represents the number of times such operators $\hat{\mathcal{H}}_C$ and $\hat{\mathcal{H}}_M$ are applied in succession on the qubits. Introducing the unitary gates U_C and U_M that depend on $(\hat{\mathcal{H}}_C, \gamma_i)$, and $(\hat{\mathcal{H}}_M, \beta_i)$, represented as:

$$U_C(\hat{\mathcal{H}}_C, \gamma_i) = \prod_i^p e^{-i\gamma_i \hat{\mathcal{H}}_C} \tag{12}$$

$$U_M(\hat{\mathcal{H}}_M, \beta_i) = \prod_i^p e^{-i\beta_i \hat{\mathcal{H}}_M} \tag{13}$$

where $\hat{\mathcal{H}}_M$ is defined as

$$\hat{\mathcal{H}}_M = \sum_{j=1}^{n} X_j. \tag{14}$$

with X_j the Pauli X operator acting on qubit j for a total of n qubits, the quantum state generated by the Ansatz reads as

$$|\Lambda(\boldsymbol{\gamma},\boldsymbol{\beta})\rangle = e^{-i\beta_p \mathcal{H}_M} e^{-i\gamma_p \mathcal{H}_C} \cdots e^{-i\beta_1 \mathcal{H}_M} e^{-i\gamma_1 \mathcal{H}_C} H|0\rangle^{\otimes n}. \tag{15}$$

A graphical representation of the Ansatz $|\Lambda(\boldsymbol{\gamma},\boldsymbol{\beta})\rangle$ is shown in Fig. 2 and in blue in the Fig. 3. Once the Ansatz has been defined, the objective function is used to guide the optimization process to find the minimum of the cost function. The objective function ϖ, instead, is defined as the expectation value of $\hat{\mathcal{H}}_C$ with respect to the parameterized quantum state

$$\varpi(\boldsymbol{\gamma},\boldsymbol{\beta}) = \langle\Lambda(\boldsymbol{\gamma},\boldsymbol{\beta})\rangle \hat{\mathcal{H}}_C |\Lambda(\boldsymbol{\gamma},\boldsymbol{\beta})\rangle. \tag{16}$$

The expectation value is the average value of all possible outcomes of the measured system. After formulating the problem into a cost Hamiltonian operator $\hat{\mathcal{H}}_C$ and Ansatz $|\Lambda(\boldsymbol{\gamma},\boldsymbol{\beta})\rangle$, the classical minimization process takes place. This procedure consists of varying the circuit parameters until the optimal set $\boldsymbol{\gamma}^\star$ and $\boldsymbol{\beta}^\star$ is found:

$$(\boldsymbol{\gamma}^\star, \boldsymbol{\beta}^\star) = \arg\min_{(\boldsymbol{\gamma},\boldsymbol{\beta})} \varpi(\boldsymbol{\gamma},\boldsymbol{\beta}). \tag{17}$$

The number of measurements needed to estimate the expectation value of a quantum state scales with the variance of the observable being measured and the desired precision. In QAOA, since the cost Hamiltonian typically consists of a sum of Pauli operators, the complexity of measuring each term grows as more qubits and deeper circuits are involved. Given that multiple Pauli terms are involved and each needs to be measured separately, the total number of measurements depends on the number of Pauli operators, the depth of the circuit, and the number of qubits. For n qubits and p layers, the number of Pauli terms typically scales as polynomial in the number of qubits, so the overall measurement complexity can be approximated as:

$$M \sim O\left(\frac{pn}{\epsilon^2}\right) \tag{18}$$

This shows that the number of measurements grows polynomially with the number of qubits and circuit depth p. A graphical representation of the QAOA is shows in Fig. 3.

IV. QAOA-Based RIS Optimization and Noise Model

QAOA is an optimization algorithm that takes advantage of the principles of quantum mechanics to explore all possible solutions in a combinatorial optimization problem. The behavior of a RIS can be described by the mathematical model reported in (5) which brings the RIS optimization a combinatorial optimization problem. This Hamiltonian is expressed directly as the sum of Pauli terms requiring no additional computational cost to decompose a matrix into Pauli summations. The number of Pauli terms, moreover, increases squared with the number of qubits according to the formula $N(N-1)/2$ that speed up the computational time. In this regard, the goal of this article is to apply QAOA in the RIS optimization to explore all the solution space to find the optimal RIS configuration that maximizes the signal reception. This approach is particularly advantageous for RIS with a high number of cells where classical optimization algorithms cannot be applied. In particular, the proposed method can be broken down into main phases, a training phase, and a testing phase. During the training phase, the quantum computational model for RIS optimization is found while the testing phase applies the trained quantum computational model to different scenarios

with different noise levels L and P different number of receiving antennas.

Phase 1: Training Phase

1) **Define the Cost Hamiltonian Operator.**
The behavior of the RIS in the optimization process is described by the SG Hamiltonian, defined in (5) considering (6) for the interactions between the cells. Considering N RIS cells, P receiving antennas and J_{ij} being an Hermitian matrix because $\xi_i^{(\tau)}\bar{\xi}_j^{(\tau)} = \overline{\xi_j^{(\tau)}\bar{\xi}_i^{(\tau)}}$, the cost Hamiltonian $\mathcal{H}_C$ can be expressed as follows:

$$\mathcal{H}_C(\boldsymbol{s}) = -\sum_{i,j}^{N} J_{ij} s_i s_j = -\sum_{i,j}^{N} \left(J_{ij} + J_{ji}\right) s_i s_j + \sum_{i}^{N} J_{ii}. \tag{19}$$

Note that even if $J_{ij}, i \neq j$, is in general complex valued, each term of the sum $J_{ij} + J_{ji} = 2J_{ij}^R$ is real and symmetric in $i \leftrightarrow j$ because it results form $\xi_i\bar{\xi}_j + \xi_j\bar{\xi}_i$. Therefore J_{ij} element is the sum of many random numbers (each one the product of two Gaussian random numbers x_i and x_j) and, for the central limit theorem, will be Gaussian distributed. Substituting (6) to (5), and mapping the variable s with the operator Z, the cost Hamiltonian reads as

$$\hat{\mathcal{H}}_C = -\frac{1}{N}\sum_{i<j}^{1,N}\sum_{\tau=1}^{P} x_i^{(\tau)} x_j^{(\tau)} Z_i Z_j \tag{20}$$

where x represents a variable from a Gaussian distribution. This Hamiltonian will be denoted as training Hamiltonian (TrH), used for the training process.

2) **Prepare the Ansatz.**
Initialize the parameterized quantum circuit $|\Lambda(\boldsymbol{\gamma}, \boldsymbol{\beta})\rangle$, which defines the variational quantum state depending on γ and β. This Ansatz is generated by applying a series of unitary operations (gates) to an initial quantum state $|0^{\otimes N}\rangle$ (all qubits in state $|0\rangle$) according to (15). The depth p of the circuit defines the number of layers of gates applied to the qubits.

3) **Evaluate the Energy of the System.**
The parameterized quantum circuit is assigned random values to the parameters, and then the state is measured. This process, denoted as quantum measurements, is repeated multiple times, in order to get an accurate expectation value of the TrH with respect to the Ansatz. This value represents the energy of the RIS configuration and represents an eigenvalue of the TrH. The related eigevector (qubit states) identifies the RIS configuration.

4) **Minimize the Energy (Classical Optimization).**
The previous step is repeated to update the values of the parameters γ and β until the minimum of the objective function in (16) is found. The classical optimization algorithm used in this study was the Broyden-Fletcher-Goldfarb-Shanno (BFGS). This algorithm is used to find the optimal values of γ and β. The algorithm runs until the minimal energy $\mathcal{H}(\boldsymbol{s})$ and related eigenvector are found. Once the optimization converges to the minimum of the objective function, the best set of parameters $\boldsymbol{\gamma}^*$ and $\boldsymbol{\beta}^*$ are found, and saved for the test phase. This nonlinear optimization method has been selected for its effectiveness in tackling unconstrained combinatorial problems, avoiding the direct computation of the Hessian, which can be computationally intensive.

Phase 2: Test Phase

1) **Assign the Optimal Parameters to the Quantum Circuit.**
Once the optimal parameters are found in the training phase, the optimal parameters $\boldsymbol{\gamma}^*$ and $\boldsymbol{\beta}^*$ are now assigned to the circuit. This circuit will be called trained circuic (TrC), that represents our trained model.

2) **Generate Test Hamiltonians.**
To test the accuracy of the TrC in finding the optimal configuration of the RIS in different electromagnetic scenarios, new cost Hamiltonians – denoted test Hamiltonians (TeHs) – are generated.

3) **Measure the State of the System.**
In order to find the optimal RIS configuration in different scenarios, the TrC is applied to all the TeHs. At this point, the minimal energies and the related RIS configurations are found, respectively. As a result of the measurements, each qubit can be in two classical states, 0 or 1, associated with the phase factor $\phi_i = -\pi$ and $\phi_i = \pi$.

4) **Apply Noise Model.** To simulate real-world EM conditions, a bit-flip noise model is implemented. This noise model adds error gates to the qubits, randomly flipping their state with a probability e_g, to account for external disturbances such as multipath fading. Different levels of noise can be tested by varying the bit-flip probability e_g, allowing an analysis of how external disturbances affect the RIS configurations.

5) **Analyze the Impact of Noise on RIS Performance.**
The effect of noise is evaluated by observing how the final RIS configurations change under varying levels of environmental noise. This step helps understand how robust the QAOA-optimized RIS is in real-world scenarios with multipath fading and other disturbances.

V. Results

A. Simulation Setup

Let's consider a wireless communication system consisting of a 3×3 matrix of 9-unit cell RIS, operating within a smart radio environment characterized by a noise level L and employing P receiving antennas. The circuit depth was $p = 18$ for a precise convergence. The behavior of the RIS has been analyzed across various EM scenarios, accounting for multipath fading, with different noise levels $L = 0, 1, 2, 3, 4$, and varying the number of receiving antennas, namely $P = 2, 4, 6, 8$. The noise levels $L = 1, \ldots, 4$ correspond to error probabilities $e_g = 0.001, 0.002, 0.003, 0.004$ of the onise model, respectively. Specifically, we investigated optimal RIS configurations in different scenarios, with and without noise, employing SG mathematical model optimized by the QAOA combinatorial optimization algorithm [23]. The QAOA has been implemented using the quantum statevector simulator provided by Qiskit [30],

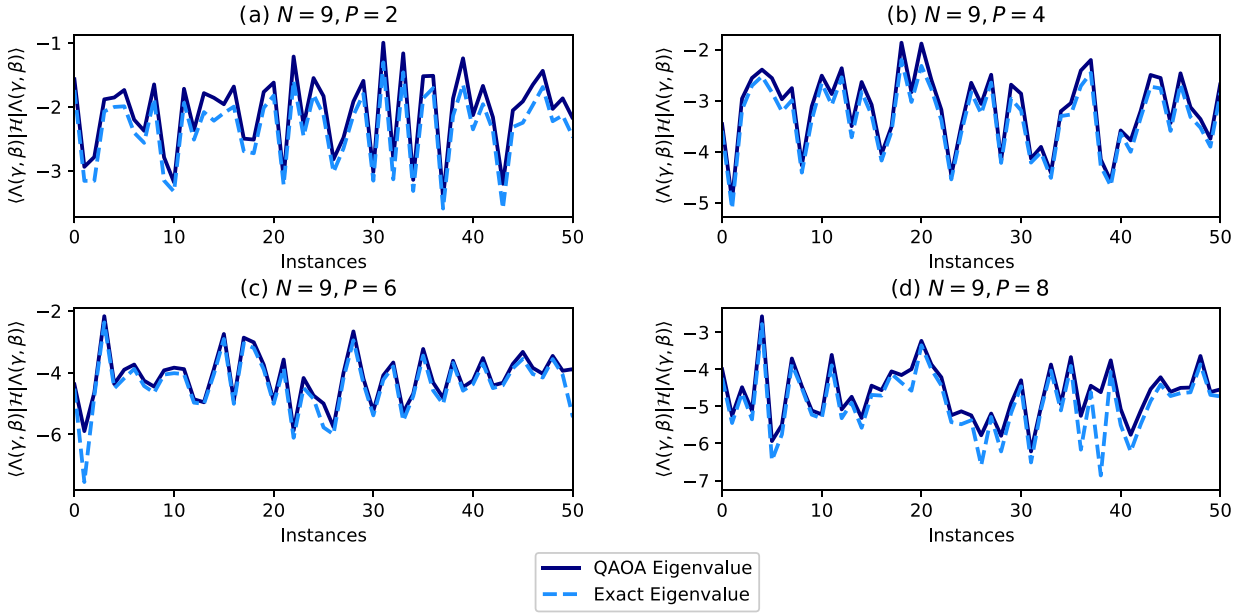

Fig. 4. Eigenvalues obtained by applying the optimizing circuit $|\Lambda(\boldsymbol{\gamma}^*, \boldsymbol{\beta}^*)\rangle$ at 50 TeH for different values of P. (a) $P = 2$, (b) $P = 4$, (c) $P = 6$ and (d) $P = 8$. The continuous line shows the eigenvalues obtained by applying the optimizing circuit and dotted line the exact ones, computed analytically.

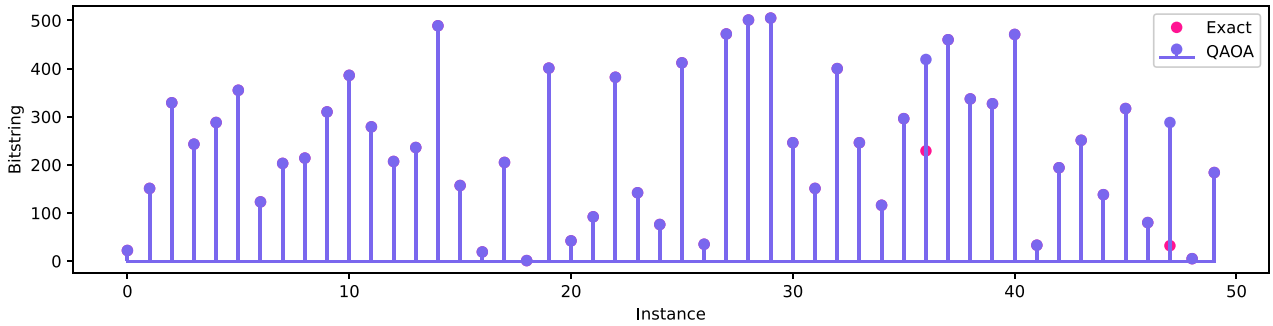

Fig. 5. Optimal bitstrings obtained by applying the optimizing circuit $|\Lambda(\boldsymbol{\gamma}^*, \boldsymbol{\beta}^*)\rangle$ at 50 TeH for $P = 2$ compared to the ones computed mathematically.

an open-source framework developed by IBM Quantum for programming quantum computers. This framework facilitates the exploration, development, and testing of quantum algorithms and applications through the IBM Quantum Cloud Platform. This allows us to emulate the behavior of NISQ systems using quantum simulators. To model quantum circuits and manage classical-quantum communication, we employed the estimator and sampler primitives available in Qiskit Runtime, ensuring seamless portability of code to IBM quantum computers without modification. Furthermore, a statevector simulator with noise has been implemented to assess the effectiveness of QAOA in optimizing RIS under various EM scenarios.

The testing phase (ThP) involves analysing the EM response of the RIS across various electromagnetic scenarios, applying the TrC obtained at the end of the training phase (TrP).

B. RIS Response in Noiseless Environments

The primary objective of this analysis is to investigate the response of a RIS in a noiseless environment without multipath fading. This involves evaluating the energies and the optimal bitstrings for different P. In this experiment, 50 instances of TeHs were generated, corresponding to 50 distinct EM scenarios. These scenarios involved varying the number of receiving antennas ($P = 2, 4, 6, 8$) while maintaining a noise level $L = 0$. The eigenvalues were obtained by applying $|\Lambda(\boldsymbol{\gamma}, \boldsymbol{\beta})\rangle$ to these 50 TeHs instances. The results were then compared to the exact analytical eigenvalues. The comparison is shown in Fig. 4, where the eigenvalues are plotted on the y-axis and the instances on the x-axis. Additionally, the bitstrings that maximize the intensity of the received signal were analyzed. For $P = 2$, the x-axis in Fig. 5 represents 9-bit sequences in decimal notation, ranging from 0 to 511, identifying the states of the RIS cells that optimize the received signal. The y-axis shows the probability at which each bitstring optimizes the scenarios. Analytical bitstrings are also included for comparison. The application of the TrC to the 50 TeHs reveals that the RIS configurations are optimal in scenarios without multipath fading. The closer the computed eigenvalues are to the analytical ones, the higher the likelihood of achieving an optimal RIS configuration. The plot in Fig. 5 reports the

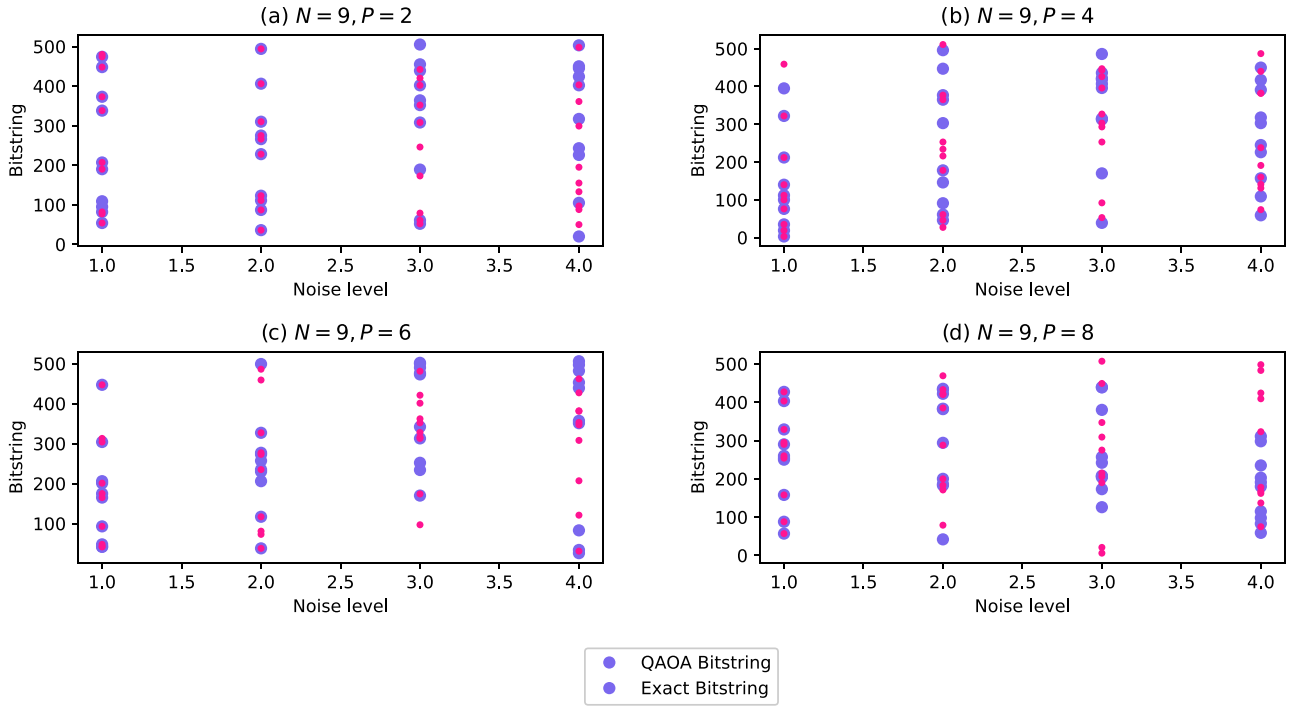

Fig. 6. Eigenvalues obtained by applying the optimizing circuit $|\Lambda(\boldsymbol{\gamma}^*, \boldsymbol{\beta}^*)\rangle$ at 50 TeH for different values of P and $L = 1, 2, 3, 4$. (a) $P = 2$, (b) $P = 4$, (c) $P = 6$ and (d) $P = 8$. The purple dots shows the bitstrings obtained by applying the optimizing circuit and pink dots the exact ones, computed mathematically.

optimal RIS configurations at 50 differenct scenarios compared to the exact one computed analytically. Overall, the analysis confirms that in the absence of noise and multipath effects, the RIS can be configured optimally by minimizing the error between computed and analytical eigenvalues and by identifying the appropriate bitstrings that maximize signal intensity.

C. RIS Response in Noisy Environments

The objective of this analysis is to study the electromagnetic response of a RIS under varying noise levels and different numbers of receiving antennas. This involves evaluating the impact of multipath fading on the RIS configuration by introducing quantum noise using a bit-flip noise model. To simulate multipath fading in a smart radio environment, quantum noise was added to the TrC. This noise was modeled using a bit-flip noise model, which introduces the Pauli X quantum gate with a certain probability e_g after the application of any gate to any qubit, simulating readout errors. The bit-flip errors considered were $e_g = 0.001, 0.002, 0.003, 0.004$, corresponding to noise levels $L = 1, 2, 3, 4$ respectively. For each noise level, 10 instances of TeHs were examined across various EM scenarios categorized by the number of receiving antennas ($P = 2, 4, 6, 8$). The optimal RIS configurations were computed and compared to analytical ones. These configurations were reported in decimal notation, representing a total of 512 potential configurations, as shown in Fig. 6. Additionally, the EM response of the RIS was analyzed for 50 TeHs at varying noise levels with a fixed number of receiving antennas ($P = 2$). The match between the computed state of the RIS cell and the ideal state was expressed in terms of qubit states and visualized in Fig. 7. If the qubit state matched the ideal state, the value reported was 1 (yellow dot); if different, the value was -1 (purple dot). The analysis demonstrates that the RIS configurations achieve high precision in noiseless scenarios and at lower noise levels ($L = 1, 2$). As noise levels increase ($L = 3, 4$), the accuracy of the optimal configurations decreases, as evidenced by a larger spread in the optimal bitstrings and a reduced number of matching bitstrings with the ideal state. Fig. 6 shows the computed optimal bitstrings contrasted with analytical ones, indicating high precision for lower noise levels and decreased accuracy as noise increases. As noise levels increase, the number of optimal configurations rises, reflecting the system's reduced ability to maintain optimal configurations under higher noise conditions. In conclusion, the electromagnetic response of the RIS is highly accurate in low-noise environments. However, as noise levels increase, the accuracy of the optimal RIS configurations diminishes, underscoring the impact of quantum noise on the RIS performance in multipath fading conditions.

D. Deep Analysis of RIS Response in a Noisy Environment

The objective of this analysis is to evaluate the effectiveness of the QAOA in optimizing the configuration of a RIS in the presence of multipath fading and varying noise levels. This is done within a single electromagnetic scenario consisting of one receiving antenna ($P = 1$). The experiment involves a single realization of disorder generated by creating a Hamiltonian for each noise level ($L = 1, 2, 3, 4$). To perform a statistical analysis of this scenario, two sets of replicas of the original system were

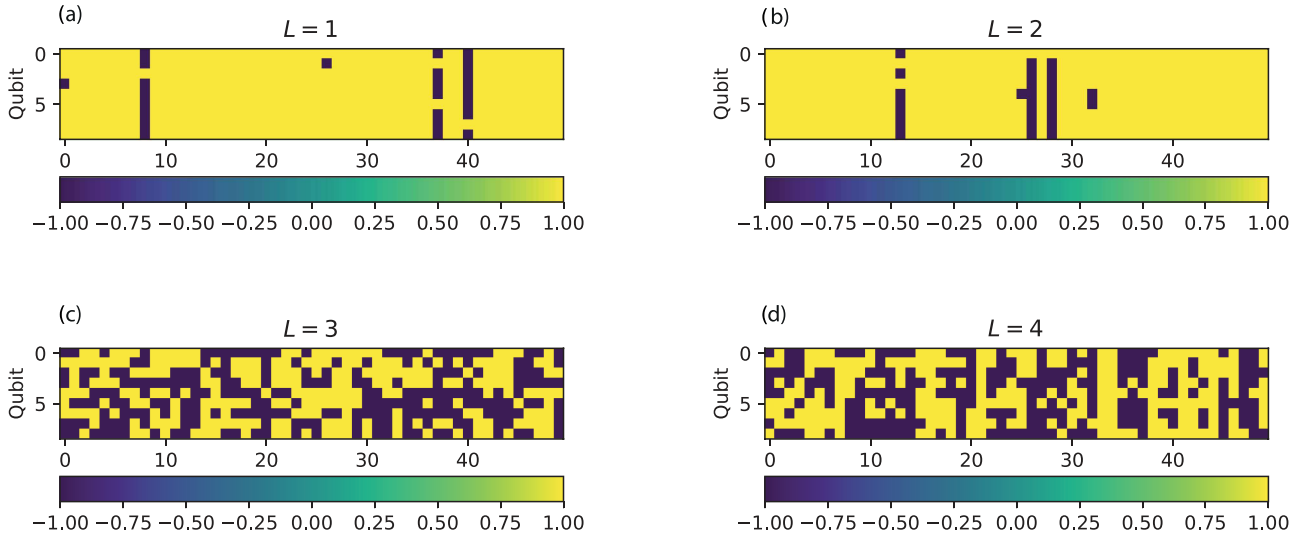

Fig. 7. Match matrices. These matrices show the match between the optimal bitstrings and the ideal ones for $P = 2$ and different levels of noise. The matrices reports 1 in case the optimal qubit state matches the ideal one, -1 in case the optimal bitstring does not match the ideal state. The results are reported for (a) $L = 1$, (b) $L = 2$, (c) $L = 3$ and (d) $L = 4$.

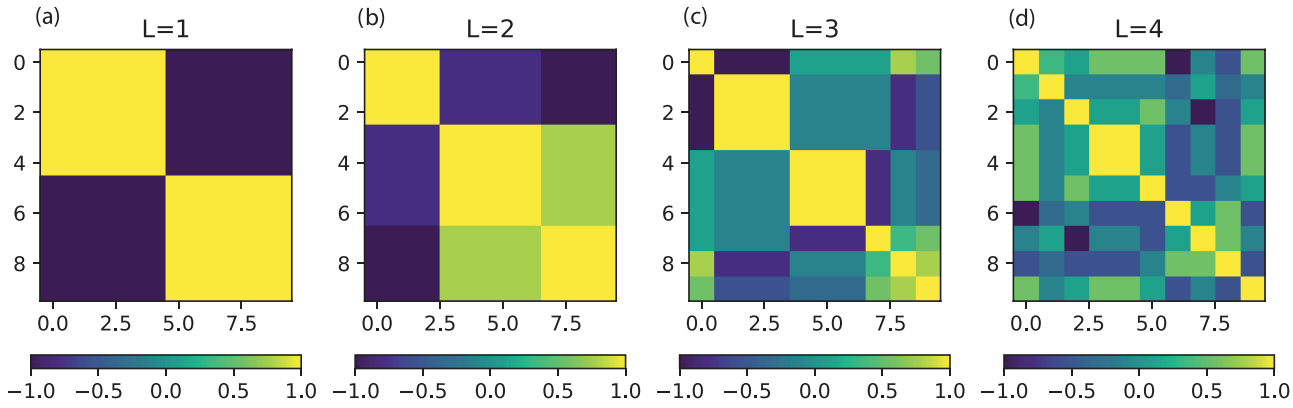

Fig. 8. Overlapping matrices for a single disorder realization at different level of noise. The overlap $q(p1, p2)$–defined in (8) –between the configurations $S(p_1)$ and $S(p_2)$ of two replicated systems and sorted by a k-means algorithm in order to be organized in clusters. In (a) the appearance of only two different yellow squares indicates that the only configurations that optimize the system are only two, perfectly anticorrelated, as a symptom of full tolerance to $L = 1$. From (b) to (d) the optimal configurations belong to an increasingly large number of clusters.

created at different noise levels, labeled as $p_1 = 1, \ldots, 10$ and $p_2 = 1, \ldots, 10$. These replicas help explore different configurations of the system and study its statistical behaviors, as the theory of SG. For a fixed noise level, the TrC was applied to the p_1 replicas and then to the p_2 replicas to determine the optimal RIS configurations. The similarity between the RIS configurations of the different replicas was measured using an overlap matrix, calculated as the normalized scalar product:

$$q(p_1, p_2) = \frac{1}{N} \boldsymbol{S}^{(p_1)} \cdot \boldsymbol{S}^{(p_2)} = \frac{1}{N} \sum_{k=1}^{N} S_k^{(p_1)} S_k^{(p_2)} \qquad (21)$$

This matrix, being symmetric and with ones on the diagonal, was visualized by sorting p_1 and p_2 using a k-means algorithm to cluster similar final S configurations. This clustering allows the states to appear as yellow squares on the overlap matrix diagonal. Fig. 8 shows the overlapping matrices for noise levels $L = 1, 2, 3, 4$. Additionally, the probability density function (PDF) of the overlap between pairs of replicas, $P(q)$, was analyzed to demonstrate the noisy behavior and degree of complexity of the system across different noise levels, as shown in Fig. 9. The analysis reveals that at a low noise level ($L = 1$), the RIS configuration shows high tolerance to noise, with only two anticorrelated optimal configurations visible in the overlap matrix (Fig. 8(a). This is expected due to the symmetry of the system, where any disordered scenario can be optimized with two anticorrelated configurations. As noise levels increase, the complexity of the system rises. For $L = 2$, more peaks appear in the PDF of the overlap (Fig. 9(b)), indicating a higher number of correlated optimal configurations due to the presence of noise. At $L = 3$, the influence of noise further increases, resulting in a higher number of non-optimal configurations, as

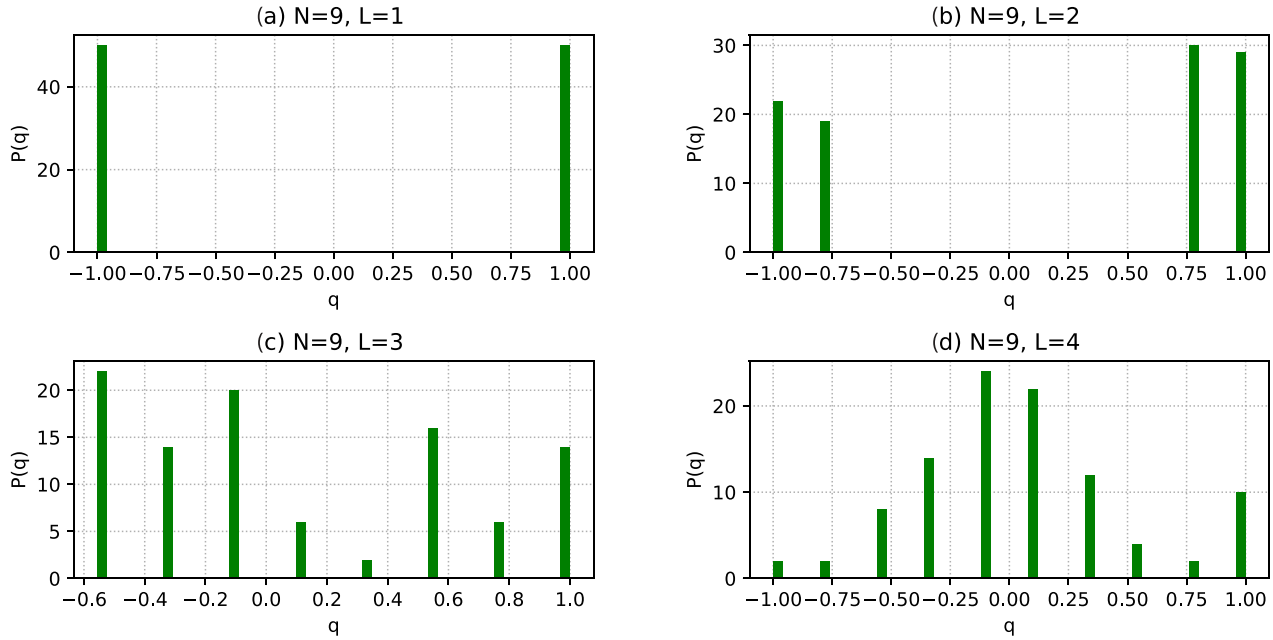

Fig. 9. Probability distribution of the overlapping matrices for $P = 1$ and different levels of noise. In (a) only two anticorrelated strings appears, as a result of all optimal configurations. In (b) only a small alteration to the optimization system stands out with just 4 optimal configurations. In (c) the noise affects the possible optimizing configurations with lower percentage while in (d) the level of noise is more relevant.

shown in Fig. 9(c). This trend continues at $L = 4$, where the probability of obtaining non-optimal configurations becomes significant, leading to a non-optimal RIS behavior (Fig. 9(d)). In summary, the effectiveness of QAOA in optimizing the RIS configuration decreases with increasing noise levels. While the RIS demonstrates high accuracy in low-noise conditions, the presence of higher noise levels results in a more complex system with a greater likelihood of non-optimal configurations. This underscores the impact of quantum noise on the performance of RIS in multipath fading conditions, highlighting the challenges in maintaining optimal configurations as noise increases.

VI. Conclusion

In conclusion, the study of the QAOA provides valuable insights into optimizing RIS in wireless communication systems. Current NISQ systems allow for an increased number of qubits in the training process, enabling the testing and validating of the algorithm in environments characterized by multipath fading, a large number of receiving antennas, and higher noise levels. Unlike classical training algorithms, QAOA does not rely on large training datasets but uses a SG mathematical model, greatly simplifying the training process. Additionally, while classical combinatorial optimization algorithms face exponential growth in RIS configurations as the number of cells increases, QAOA only experiences a polynomial increase in complexity, making it suitable for solving large-scale problems [40]. Our simulations and analysis across various EM scenarios have demonstrated the efficacy of QAOA in identifying optimal RIS configurations, even in the presence of challenges like multipath fading and noise. In noiseless scenarios, QAOA effectively identified optimal RIS configurations, maximizing received signal intensity and minimizing data loss. The comparison between computed and analytical eigenvalues highlights the accuracy and reliability of QAOA-optimized configurations. Even as noise levels increase, QAOA continues to perform commendably, showcasing its adaptability and robustness. Furthermore, analysis of RIS behavior in the presence of multipath fading reveals promising results. Despite the added complexity introduced by multipath fading, QAOA continues to exhibit effectiveness in optimizing RIS configurations. While the accuracy may decrease slightly with significant multipath fading, the overall performance remains commendable across various scenarios. These findings highlighted the potential of quantum computing, particularly QAOA, in addressing the complexities associated with RIS optimization in wireless communication systems. By leveraging the computational power of quantum algorithms, we can overcome traditional limitations and unlock new possibilities for enhancing the performance and reliability of wireless networks. For this study, we chose to start with a simpler single input and multiple output (SIMO) system to showcase the potential advantages of QAOA-based optimization in smart radio environments. The SIMO configuration allows for easier implementation and more direct benchmarking, providing examples of how quantum techniques could potentially improve RIS performance. In further study, the extension of the QAOA approach to MIMO systems can be performed by adapting the SG Hamiltonian for multiple input scenarios, including contributions from all transmitting and receiving antennas and resulting in a more sophisticated model for quantum optimization. Moreover, as the system size grows, simulating quantum algorithms like QAOA becomes computationally infeasible due to this exponential scaling. In fact, in quantum hardware the computational complexity grows polynomially in the number of qubits n while in classical

hardware exponentially. This scaling problem makes simulators used for validating the algorithm impractical for large systems. For this reason, further research and experimentation are essential to refine and validate the algorithm in real quantum computers, increasing significantly the system size. Despite the important features brought by the quantum optimization, the QAOA relies on current NISQ devices, prone to noise, qubit errors, and limited coherence times, which can affect the accuracy of computations. As the complexity of the problem increases, quantum noise may degrade the performance of QAOA while the number of quantum measurement increases polinomially. Large-scale optimization problems require a high number of qubits, which are currently limited in available quantum hardware. This restricts the size of the RIS system that can be optimized. While the quantum part of QAOA handles the combinatorial optimization problems efficiently, the classical optimization of parameters γ and β can become computationally expensive as the number of qubits or circuit depth increases. In this regard, to overcome such QAOA limitations in classical hardware, implementation of QAOA on NISQ systems is essential. In order to reduce the impact of noise, techniques like quantum error correction or error mitigation strategies can be applied. Techniques such as grouping Pauli operators and shot frugality can instead be used to reduce the number of quantum measurements, while more efficient gradient-based or quantum-inspired optimization algorithms can be used to speed up the system training process. In case of simulations of quantum simulators, other noise models can be explored to see the difference of RIS responses and optimize the model for real world implementation. Following these improvements, quantum-based RIS optimization can become significantly interesting by providing important improvements to RIS performance, enhancing wireless communication systems.

REFERENCES

[1] A. Goldsmith, *Wireless Communications*. Cambridge, U.K.: Cambridge Univ. Press, 2005.

[2] A. F. Molisch, *Wireless Communications*. Hoboken, NJ, USA: Wiley, 2012.

[3] D. J. Love, R. W. Heath, V. K. Lau, D. Gesbert, B. D. Rao, and M. Andrews, "An overview of limited feedback in wireless communication systems," *IEEE J. Sel. Areas Commun.*, vol. 26, no. 8, pp. 1341–1365, Oct. 2008.

[4] G. Gradoni and M. Di Renzo, "Smart radio environments," *Rev. Electromagnetics*, vol. 1, pp. 1–42, 2022.

[5] J. D. Parsons, *Mobile Communication Systems*. Berlin, Germany: Springer Science and Business Media, 2012.

[6] L. Lanbo, Z. Shengli, and C. Jun-Hong, "Prospects and problems of wireless communication for underwater sensor networks," *Wirel. Commun. Mobile Comput.*, vol. 8, no. 8, pp. 977–994, 2008.

[7] M. Colombo et al., "Experimental investigation of 5G base station functionalities in reverberation chamber at millimeter-wave," *IEEE Access*, vol. 11, pp. 121702–121711, 2023.

[8] E. Basar, M. Di Renzo, J. De Rosny, M. Debbah, M.-S. Alouini, and R. Zhang, "Wireless communications through reconfigurable intelligent surfaces," *IEEE Access*, vol. 7, pp. 116753–116773, 2019.

[9] G. C. Alexandropoulos et al., "Ris-enabled smart wireless environments: Deployment scenarios, network architecture, bandwidth and area of influence," *EURASIP J. Wireless Commun. Netw.*, vol. 2023, no. 1, Art. no. 103, 2023.

[10] C. Ross, G. Gradoni, Q. J. Lim, and Z. Peng, "Engineering reflective metasurfaces with ising Hamiltonian and quantum annealing," *IEEE Trans. Antennas Propag.*, vol. 70, no. 4, pp. 2841–2854, Apr. 2022.

[11] Q. J. Lim, C. Ross, A. Ghosh, F. W. Vook, G. Gradoni, and Z. Peng, "Quantum-assisted combinatorial optimization for reconfigurable intelligent surfaces in smart electromagnetic environments," *IEEE Trans. Antennas Propag.*, vol. 72, no. 1, pp. 147–159, Jan. 2024.

[12] C. Ross, G. Gradoni, and Z. Peng, "A hybrid classical-quantum computing framework for ris-assisted wireless network," in *Proc. 2023 IEEE IEEE MTT-S Int. Conf. Numer. Electromagn. Multiphys. Model. Optim.*, 2023, pp. 99–102.

[13] G. Gradoni et al., "Smart radio environments," 2021, [Online]. Available: https://arxiv.org/abs/2111.08676

[14] L. Bastianelli et al., "Measurements of reconfigurable intelligent surface in 5G system within a reverberation chamber at MmWave," pp. 1–4, 2024, doi: 10.23919/EuCAP60739.2024.10501507.

[15] E. Colella, L. Bastianelli, F. Moglie, and V. M. Primiani, "Near field optimization algorithm for reconfigurable intelligent surface," in *Proc. 35th IEEE Gen. Assem. Sci. Symp. Int. Union Radio Sci.*, 2023, pp. 1–4.

[16] Z. Li et al., "Phase shift design in RIS empowered wireless networks: From optimization to ai-based methods," *Network*, vol. 2, no. 3, pp. 398–418, 2022.

[17] H. Zhou, M. Erol-Kantarci, Y. Liu, and H. V. Poor, "A survey on model-based, heuristic, and machine learning optimization approaches in ris-aided wireless networks," *IEEE Commun. Surv. Tut.*, vol. 26, no. 2, pp. 781–823, Secondquarter 2024.

[18] G. Parisi, "Magnetic properties of spin glasses in a new mean field theory," *J. Phys. A: Math. Gen.*, vol. 13, no. 5, 1980, Art. no. 1887.

[19] M. Mézard, G. Parisi, and M. A. Virasoro, "Toward a mean field theory for spin glasses," *Phys. Lett. A*, vol. 73, no. 3, pp. 203–205, 1979.

[20] M. Mézard, G. Parisi, and M. A. Virasoro, *Spin Glass Theory and Beyond: An Introduction to the Replica Method and Its Applications*. Singapore: World Scientific Publishing Company, 1987.

[21] K. H. Fischer and J. A. Hertz, *Spin Glasses*. Cambridge, U.K: Cambridge Univ. Press, 1993.

[22] A. P. Young, *Spin Glasses and Random Fields*. Singapore: World Scientific, 1998.

[23] M. Leonetti, E. Hörmann, L. Leuzzi, G. Parisi, and G. Ruocco, "Optical computation of a spin glass dynamics with tunable complexity," *Proc. Nat. Acad. Sci.*, 2021, vol. 118, no. 21, Art. no. e2015207118.

[24] A. Steane, "Quantum computing," *Rep. Prog. Phys.*, vol. 61, no. 2, 1998, Art. no. 117.

[25] M. Hirvensalo, *Quantum Computing*. Berlin, Germany: Springer Science Business Media, 2003.

[26] E. Grumbling and M. Horowitz, *Quantum Computing: Progress and Prospects*. Washington, DC, USA: The National Academies Press, 2019.

[27] M. Brooks, What's next for quantum computing. 2023. [Online]. Available: https://www.technologyreview.com/2023/01/06/1066317/whats-next-for-quantum-computing/

[28] M. Cerezo et al., "Variational quantum algorithms," *Nature Rev. Phys.*, vol. 3, no. 9, pp. 625–644, 2021.

[29] J. R. McClean, J. Romero, R. Babbush, and A. Aspuru-Guzik, "The theory of variational hybrid quantum-classical algorithms," *New J. Phys.*, vol. 18, no. 2, Feb. 2016, Art. no. 023023. [Online]. Available: https://doi.org/10.10882F1367-26302F182F22F023023

[30] S. Endo, Z. Cai, S. C. Benjamin, and X. Yuan, "Hybrid quantum-classical algorithms and quantum error mitigation," *J. Phys. Soc. Jpn.*, vol. 90, no. 3, 2021, Art. no. 032001.

[31] E. Colella, S. Beloin, L. Bastianelli, V. M. Primiani, F. Moglie, and G. Gradoni, "Variational quantum shot-based simulations for waveguide modes," *IEEE Trans. Microw. Theory Techn.*, vol. 72, no. 4, pp. 2084–2094, Apr. 2024, doi: 10.1109/TMTT.2023.3339243.

[32] L. Zhou, S.-T. Wang, S. Choi, H. Pichler, and M. D. Lukin, "Quantum approximate optimization algorithm: Performance, mechanism, and implementation on near-term devices," *Phys. Rev. X*, vol. 10, no. 2, 2020, Art. no. 021067.

[33] E. Farhi, J. Goldstone, S. Gutmann, and L. Zhou, "The quantum approximate optimization algorithm and the Sherrington-Kirkpatrick model at infinite size," *Quantum*, vol. 6, 2022, Art. no. 759.

[34] E. Colella, L. Bastianelli, M. Khalily, F. Moglie, Z. Peng, and G. Gradoni, "Quantum optimisation of reconfigurable surfaces in complex propagation environments," in *Proc. 18th Eur. Conf. Antennas Propag.*, Glasgow, United Kingdom, 2024, pp. 1–5.

[35] C. W. Beenakker, "Random-matrix theory of quantum transport," *Rev. Modern Phys.*, vol. 69, no. 3, 1997, Art. no. 731.

[36] J. J. Hopfield, "Neural networks and physical systems with emergent collective computational abilities," *Proc. Nat. Acad. Sci.*, 1982, vol. 79, no. 8, pp. 2554–2558.

[37] D. J. Amit, H. Gutfreund, and H. Sompolinsky, "Spin-glass models of neural networks," *Phys. Rev. A*, vol. 32, no. 2, 1985, Art. no. 1007.
[38] G. Gradoni, S. Terranova, Q. J. Lim, C. Ross, and Z. Peng, "Random ising Hamiltonian model of metasurfaces in complex environments," in *Proc. 17th IEEE Eur. Conf. Antennas Propag.*. 2023, pp. 1–5.
[39] M. A. Nielsen and I. L. Chuang, *Quantum Computation and Quantum Information*. Cambridge, U.K.: Cambridge Univ. Press, 2010.
[40] E. Farhi, J. Goldstone, and S. Gutmann, "A quantum approximate optimization algorithm," 2014, arXiv:1411.4028.

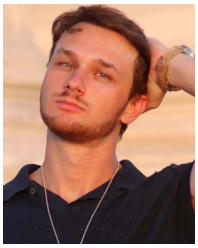

Emanuel Colella (Graduate Student Member, IEEE) received the Bachelor's of Science degree and Master's with distinction (cum laude) degree in biomedical engineering from the UniversitÃ Politecnica delle Marche, Ancona, Italy, in 2015 and 2019, respectively. He currently a Biomedical Engineer. In 2020, he joined the National Inter-University Consortium for Telecommunications as a Researcher for the RISE-6G project, where he conducted computational electrodynamic simulations of Reconfigurable Intelligent Surfaces to assess their performance in smart radio environments. In 2022, he was appointed project lead for working group P2718, focusing on the characterization of unintentional stochastic radiators. Colella commenced the Ph.D. in 2022, specializing in electromagnetic analysis of complex structures using both classical and quantum algorithms. In 2023, he became the Principal investigator for a unique cooperative research and development agreement between the Naval Surface Warfare Center, Dahlgren Division), University of Surrey, and the UniversitÃ Politecnica delle Marche, specifically focusing on Quantum Computational Electromagnetics.

Luca Bastianelli (Member, IEEE) received the M.S. degree in electronic engineering from Università Politecnica delle Marche, Ancona, Italy, and the Ph.D. degree in biomedical, electronics and telecommunication engineering from Università Politecnica delle Marche, Ancona, Italy, in 2018. In 2018, he was a Research Fellow with the Dipartimento di Ingegneria dell'Informazione, Università Politecnica delle Marche. He is currently a Researcher with the CNIT at the Dipartimento di Ingegneria dell'Informazione, Università Politecnica delle Marche. He is involved in the area of electromagnetic compatibility, telecommunications and computational electrodynamics. His research interests include reverberation chambers, wave chaos, propagation in complex systems, ray tracing, time reversal, metasurfaces, 5G and numerical techniques on high performance computers. He was a Member of the COST Action IC1407 ACCREDIT. He was involved in many PRACE projects and he currently lead the FDTDLIME project on reconfigurable intelligent surfaces. He is currently a active Member of the Working Group for the development of the IEEE Std P2718 on near field characterization. He is currently involved in the H2020 RISE-6G project. During the Ph.D. degree, he spent seven months with the University of Nottingham, Nottingham, U.K. During his Fellowship he is involved in teaching support activities. He was the recipient of the URSI Commission E Young Scientist Award in 2017.

Valter Mariani Primiani (Senior Member, IEEE) received the Laurea degree (summa cum laude) in electronic engineering from the University of Ancona, Ancona, Italy, in 1990. He is currently a Professor in electromagnetic compatibility with the Università Politecnica delle Marche, Ancona, Italy. He is a Member with the Department of Information Engineering, where he is also responsible for the EMC Laboratory. His research interests include the prediction of digital printed circuit board radiation, the radiation from apertures, the electrostatic discharge coupling effects modeling, and the analysis of emission and immunity test methods. Since 2003, he has been also involved in research activities on the application of reverberation chambers for compliance testing and for metrology applications. He is currently a Member of the COST Action 1407 ACCREDIT on the characterization of stochastic emissions from digital equipment. He is a Senior Member of the IEEE (EMC society) and a Member of the Italian Society of Electromagnetics. From 2007 to 2013, he was a active Member of the Working Group for the development of the IEEE Std 299.1-2013 on shielding effectiveness measurements. Since 2021, he was been involved in the RISE–6G project. Since 2014, he has been a Member of the International Steering Committee of EMC Europe. He is currently an Associate Editor of the journal IET Science, Measurement and Technology. He is in the World's Top 2% Scientists by Elsevier, November 2023.

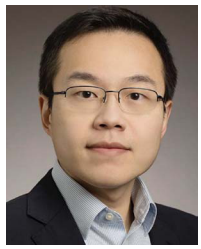

Zhen Peng (Senior Member, IEEE) received the B.S. degree in electrical engineering and information science from the University of Science and Technology of China, Hefei, China, in 2003, and the Ph.D. degree in electromagnetics and microwave engineering from the Chinese Academy of Science, Beijing, China, in 2008. From 2008 to 2013, he was with the ElectroScience Laboratory, The Ohio State University, Columbus, OH, USA, first as a Postdoctoral Fellow from 2008 to 2009 and then as a Senior Research Associate from 2010 to 2013. From 2013 to 2019, he was an Assistant Professor with the Department of Electrical and Computer Engineering, The University of New Mexico, Albuquerque, NM, USA. He is currently an Associate Professor with the Department of Electrical and Computer Engineering (ECE ILLINOIS), University of Illinois with Urbana–Champaign, Champaign, IL, USA. His research interests include computational, statistical, and applied electromagnetics. The goal is to simulate classical and quantum electrodynamic physics with intelligent algorithms on state-of-theart computers, where virtual experiments can be performed for the prediction, discovery, and design of complex systems with unprecedented scales. His research work has an impact on both the civilian and commercial engineering applications, including advanced antennas, radio frequency integrated circuits, electromagnetic interference and compatibility, signal and power integrity, and wireless communication. He was the recipient of the 30th Conference on Electrical Performance of Electronic Packaging and Systems) Best Paper Award in 2021, the IEEE ELECTROMAGNETIC COMPATIBILITY, Symposium Best Paper Award in 2019, National Science Foundation CAREER Award in 2018, Best Transaction Paper Award--IEEE TRANSACTIONS ON COMPONENTS, PACKAGING AND MANUFACTURING TECHNOLOGY in 2018, IEEE Albuquerque Section Outstanding Young Engineer Award in 2017, UNM Electrical and Computer Engineering Department's Distinguished Researcher Award in 2016, Applied Computational Electromagnetics Society) Early Career Award in 2015, IEEE Antenna and Propagation Sergei A. Schelkunoff Transactions Prize Paper Award in 2014, a number of young scientist awards, and an advisor of best student paper awards from various conferences.

Franco Moglie (Senior Member, IEEE) received the "Dottore Ingegnere" degree in electronics engineering from the University of Ancona, Ancona, Italy, in 1986, and the Ph.D. degree in electronics engineering and electromagnetics from the University of Bari, Bari, Italy, in 1992. Since 1986, he has been a Research Scientist with the Università Politecnica delle Marche, Ancona, Italy, and since 2011, he has been with the Department of Information Engineering. Since 2016, he has been an Associate Professor with the Università Politecnica delle Marche, Ancona, Italy. His research interests include EM numerical techniques. In particular, his research activity is in the field of the application of reverberation chambers for compliance testing, metrology applications, and multipath propagation. In 2011, he was a visiting Researcher with Wave Chaos Group, IREAP, University of Maryland, College Park, MD, USA. From 2013 to 2019, he led three PRACE high performance computing projects on reverberation chambers. Since 2014, he has been an Italian management committing Member of the COST Action IC1407. From 2007, he is or was an active Member of some Working Groups for the development of IEEE Standards: 299.1, 1302, 2715, and 2716. Since 2017, he has been a secretary of the working group for the IEEE Standard 2718. Since 2007, he has been a Member of the "Accademia Marchigiana di Scienze, Lettere ed Arti – Istituto Culturale Europeo" (Marches Academy of Sciences, Arts and Letters – European Cultural Institute), which is based in Ancona. Since 2021, he has been the scientific Manager for CNIT with Università Politecnica delle Marche in the RISE–6G project. He is a Member of the IEEE Electromagnetic Compatibility Society and the Italian Electromagnetics Society. In 2013, he was the recipient of the title of Distinguished Reviewer of theIEEE TRANSACTIONS ON ELECTROMAGNETIC COMPATIBILITY. He is in the World's Top 2% Scientists by Elsevier, 2023.

Gabriele Gradoni (Senior Member, IEEE) received the Ph.D. degree in electromagnetics from the Università Politecnica delle Marche, Ancona, Italy, in 2010. He was a Visiting Researcher with the Time, Quantum, and Electromagnetics Team, National Physical Laboratory, Teddington, U.K., in 2008. From 2010 to 2013, he was an Research Associate with the Institute for Research in Electronics and Applied Physics, University of Maryland, College Park, MD, USA. From 2013 to 2016, he was a Research Fellow with the School of Mathematical Sciences, University of Nottingham, Nottingham, U.K. Since 2023 he has been a Full Professor of mathematics and electrical engineering with the University of Nottingham, U.K. His research interests include probabilistic and asymptotic methods for propagation in complex wave systems, wave chaos, and metasurfaces, with applications to electromagnetic compatibility and modern wireless communication systems. He is a Member of the American Physical Society, and the Italian Electromagnetics Society. He was the recipient of the URSI Commission B Young Scientist Award in 2010 and 2016, Gaetano Latmiral Prize in 2015, Honorable Mention IEEE TEMC Richard B. Schulz Transactions Prize Paper Award in 2020, and the EuCAP Best Electromagnetics Paper Award in 2021. From 2014 to 2021, he has been the URSI Commission E Early Career Representative. Since 2020, he has been a Royal Society Industry Fellowwith British Telecommunications, London, U.K., and an Adjunct Associate Professor with the Department of Electrical and Computer Engineering, University of Illinois Urbana Champaign, Champaign, IL, USA Since 2022 he has been a Visiting Fellow with the Department of Computer Science and Technology, University of Cambridge, Cambridge, U.K.